

# What does DQE say about lesion detectability in digital radiography?

Angel R. Pineda <sup>\*ab</sup> and Harrison H. Barrett <sup>\*\*abc</sup>

<sup>a</sup>Department of Radiology, University of Arizona

<sup>b</sup>Program in Applied Mathematics, University of Arizona

<sup>c</sup>Optical Sciences Center, University of Arizona

## ABSTRACT

Currently, there is significant interest in quantifying the performance of digital radiography systems. Digital radiography systems can be thought of as continuous linear shift-invariant systems followed by sampling. This view, along with the large number of pixels used for flat-panel systems, has motivated much of the work which attempts to extend figures of merit developed for analog systems, in particular, the detective quantum efficiency (DQE) and the noise equivalent quanta (NEQ). A more general approach looks at the system as a continuous-to-discrete mapping and evaluates the signal-to-noise ratio (SNR) completely from the discrete data. In this paper, we study the effect of presampling blur on these figures of merit. We find that even in this idealized model the DQE/NEQ formulations do not accurately track the behavior of the fully digital SNR. Therefore, DQE/NEQ cannot be viewed as indicators of the signal-known-exactly/background-known-exactly (SKE/BKE) detectability. In order to make design decisions by optimizing detectability one must work with the fully digital definition of detectability.

**Keywords:** Image quality, detectability, digital radiography, DQE, NEQ, SNR

## 1. INTRODUCTION

Conventional wisdom regarding the evaluation of digital radiography centers around DQE formulations that combine the digital and continuous aspects of the imaging system.<sup>1-5</sup> These expressions are an attempt to provide a frequency-dependent signal-to-noise ratio (SNR) that can be used to optimize the hardware of the imaging system. These DQE formulations are being used to make design decisions such as the preferred amount of presampling blur.<sup>4,6</sup> In these studies it has been found that some presampling blur not only reduces aliasing but that it may increase the SNR.

In analog radiography systems with a stationary and linear shift-invariant (LSIV) model, one can decompose the SNR into a hardware component and an object component.<sup>7,8</sup> The DQE gives the hardware-dependent part of the SNR. Hence, by optimizing the DQE, one can optimize the hardware independent of the object to be imaged. Both the separation of the object and hardware parts and the form of the DQE depend on the fact that the Fourier transform diagonalizes both the system operator for a LSIV system and the autocovariance function for a stationary random process. There is no such transformation that we are aware of for the digital case.

The lack of a single basis for the data that diagonalizes both the deterministic and stochastic descriptions of the system leads to different formulations for the DQE. Using a large number of pixels as a surrogate for a continuous representation of the data, one can estimate quantities analogous to the noise power spectrum (NPS) and the modulation transfer function (MTF). We are interested in validating the meaning of these formulations of the DQE by comparing them to the ideal-observer SNR computed from the data.

## 2. NEQ FOR LSIV SYSTEMS WITH STATIONARY NOISE

If we consider the analog continuous-to-continuous radiography system, we can phrase the SNR as the performance of the ideal observer in discriminating between the following two hypotheses:

$$\begin{aligned}g_0(x) &= \mathcal{H}b(x) + n, \\g_1(x) &= \mathcal{H}b(x) + \mathcal{H}s(x) + n,\end{aligned}\tag{1}$$

---

\*pineda@math.arizona.edu; phone 1 520 626 4267; fax 1 520 626 2892; Radiology Research Bldg. 211, Arizona Health Sciences Center, 1609 N. Warren, Tucson, AZ 85724; \*\*barrett@radiology.arizona.edu; phone 1 520 626 6815

where  $g_i$  represents the data under the  $i^{th}$  hypothesis,  $\mathcal{H}$  is the system operator,  $b$  is the background,  $n$  is the noise and  $s$  is the signal (in object space) to be detected. For the following analysis, we will assume the background is fixed and the signal is deterministic, low contrast and known, in other words, the signal known exactly/background known exactly (SKE/BKE) detection task where the signal does not affect the data statistics.

If we assume a Gaussian noise model, the ideal observer is the Hotelling<sup>9</sup> observer, and its performance can be expressed as:

$$SNR^2(ideal) = \int \Delta\bar{g}^*(x) [K_g^{-1} \Delta\bar{g}](x) dx, \quad (2)$$

where  $\Delta\bar{g}$  is the mean data generated by the signal and  $K_g$  is the autocovariance operator.

If we assume that the system is LSIV and we represent  $g$  in the Fourier basis, then we can write  $\Delta\bar{g}$  as:

$$\Delta\bar{g}(\nu) = G \text{OTF}(\nu) S(\nu), \quad (3)$$

where  $\nu$  is the frequency variable,  $G$  is the gain and the  $\text{OTF}$  is the optical transfer function.

If the data  $g$  is a sample of a stationary random process, then the same change of basis diagonalizes the autocovariance function:

$$\begin{aligned} K_g(x, x') &= K_g(x - x'), \\ F\{K_g(x - x')\}F^\dagger &= NPS(\nu) \delta(\nu - \nu'), \end{aligned} \quad (4)$$

where  $F$  is the Fourier transform and  $NPS$  is the noise power spectrum. We see that a single change of basis diagonalizes both operators, and we can rewrite our expression of the SNR in terms of the frequency variable:

$$SNR^2(ideal) = \int \frac{G^2 \text{MTF}^2(\nu)}{NPS(\nu)} |S(\nu)|^2 d\nu, \quad (5)$$

where the  $\text{MTF}$  is  $|\text{OTF}|$ . From this representation we can decompose the SNR expression into a hardware component and an object component. The NEQ is the hardware component<sup>7</sup>:

$$NEQ(\nu) = \frac{G^2 \text{MTF}^2(\nu)}{NPS(\nu)}. \quad (6)$$

The NEQ is a frequency-dependent SNR that does not depend on the object characteristics. If one optimizes the NEQ at all frequencies, the system has been optimized for all objects in an SKE/BKE detection task.

### 3. DISCRETE FORMULATIONS OF THE NEQ & DQE

Digital radiography systems can be seen as a continuous LSIV system followed by sampling. This view motivates attempting to extend the NEQ defined for the continuous system to the discrete case. In this case what we have is a continuous-to-discrete mapping:

$$\begin{aligned} \Delta g_i &= \int h_i(x) s(x) dx + n_i, \\ \Delta \mathbf{g} &= \mathcal{H} s(x) + \mathbf{n}, \end{aligned} \quad (7)$$

where the  $h_i$  are the sensitivity functions. It will be of some importance to note that the data and the object live in different spaces.

We first look at approximating the noise power spectrum as the sample average of periodograms of images containing noise  $\{N\}$  only:

$$NPS_d(\nu_i) = \frac{1}{M} \sum_{j=1}^M |DFT(N_j)_i|^2. \quad (8)$$

This expression of  $NPS_d(\nu_i)$  is an approximation to the variance of  $DFT(N)_i$ . While there are several experimental approaches for estimating the  $NPS$  for two-dimensional images, they are all based on this formulation. The  $NPS_d$  is defined on data space and is constrained to the discrete frequencies that can be estimated from the pixels.

The full continuous-to-discrete imaging system is not shift-invariant, and this provides a difficulty in computing an analogous quantity to the  $MTF$ . Even if we ignore the effects at the boundary, the point response varies with the location of the point with respect to the pixel. If we have a small amount of presampling blur, a point source in the middle of a pixel would result in all the photons being collected by the same pixel. If, on the other hand, the point is between two pixels, the photons would be equally divided into the two adjoining pixels. This shift variance is naturally more important for small objects than for objects that are significantly larger than a pixel.

One attempt at resolving this issue is using the  $MTF$  of the system before sampling, the presampling  $MTF$  ( $PSMTF$ ). Viewing the system as a deterministic blur of the secondary light photons or charge produced by the x-ray photons followed by convolution with the pixel functions leads to a  $PSMTF$  of the following form:

$$PSMTF(\nu) = MTF_{blur}(\nu) |\Delta x \text{sinc}(\Delta x \nu)|, \quad (9)$$

where  $\Delta x$  is the pixel width. The  $NEQ$  under this formulation would involve sampling the  $PSMTF$  at the frequencies estimated from the pixel values:

$$NEQ_d(PSMTF) = \frac{G^2 PSMTF(\nu_i)^2}{NPS_d(\nu_i)}. \quad (10)$$

We note that under this definition of  $NEQ_d$  the numerator is a continuous function (though evaluated at discrete points) and the denominator is discrete.

Another proposed alternative to remove the shift-variance introduced by the pixel is to compute an ensemble- $MTF$  ( $EMTF$ ) where one computes the data for many point locations within a pixel<sup>3</sup>:

$$\begin{aligned} MTF_j &= \Delta x |DFT\{\mathcal{H}\delta(x - x_j)\}|, \\ EMTF &= \frac{1}{M} \sum_{j=1}^M MTF_j. \end{aligned} \quad (11)$$

The  $NEQ$  under this formulation is given by:

$$NEQ_d(EMTF) = \frac{EMTF(\nu_i)^2}{NPS_d(\nu_i)}. \quad (12)$$

This approach avoids the theoretical issues of combining continuous and discrete quantities in the definition of the  $NEQ_d$ .

The  $DQE$  is the ratio of the  $SNR$  of the output of an imaging system over the  $SNR$  of the input. In terms of the  $NEQ$ , the  $DQE$  is a normalized version of the  $NEQ$ . For this paper, we will assume that the input to the imaging system is a Poisson random process with mean  $b(x) = q$ ; In physical terms, we assume a uniform background with the x rays emitted with a constant fluence of  $q$ . In this case, the  $DQE$  based on the  $PSMTF$  for the system is defined as<sup>5</sup>:

$$DQE_d(\nu_i) = \frac{q G^2 PSMTF^2(\nu_i)}{NPS_d(\nu_i)}. \quad (13)$$

#### 4. SNR FORMULATIONS

Under the approximation that the discrete data uncertainty is well described by a Gaussian probability density, the ideal observer defined from the data yields:

$$SNR^2(ideal, L) = \sum_{i=1}^N \Delta \bar{g}_i [K_g^{-1} \Delta \bar{g}]_i, \quad (14)$$

where  $\Delta \bar{g}$  is the mean difference in the data produced by the signal and  $K_g^{-1}$  is the inverse of the data covariance matrix. Note that this formulation depends on the location of the signal. To obtain an expression that is independent of the signal location, we can average over locations within a pixel:

$$\langle SNR^2(ideal) \rangle = \frac{1}{N_L} \sum_{i=1}^{N_L} SNR^2(ideal, L_i). \quad (15)$$

Both SNR formulations of the  $NEQ_d(\nu)$  provide a frequency-dependent figure of merit. In terms of ranking or optimizing imaging systems, we need to reduce them to a scalar. One way to reduce the  $NEQ_d(\nu)$  to a scalar is to weight the importance of every frequency the same and formulate the overall SNR of the system as:

$$SNR^2(NEQ_d, \delta) = \sum_{\nu_i = \frac{-1}{2\Delta x}}^{\frac{1}{2\Delta x}} NEQ_d(\nu_i) \Delta\nu. \quad (16)$$

This SNR is the area underneath the NEQ curve. If, on the other hand, we are interested in a signal of a particular size, we can weight each frequency by the frequency content of the signal of interest:

$$SNR^2(NEQ_d, S) = \sum_{\nu_i = \frac{-1}{2\Delta x}}^{\frac{1}{2\Delta x}} NEQ_d(\nu_i) |S(\nu_i)|^2 \Delta\nu. \quad (17)$$

A different type of SNR that eliminates the spatial dependence by averaging over a pixel uses a discrete-space Fourier transform (DSFT) interpretation for the  $NPS_d$  estimated from the data using a DFT.<sup>10</sup> This definition of SNR approximates the  $\langle SNR^2(ideal) \rangle$  for the case of an infinite detector and when the  $NPS_d$  can be appropriately estimated from the data.

$$SNR^2(NEQ_d, S, DSFT) = \sum_{\nu_i = -\infty}^{\infty} NEQ_d(\nu_i) |S(\nu_i)|^2 \Delta\nu. \quad (18)$$

For an analytic approach to estimating the  $NPS_d$  in simulation, see Clarkson, et. al.<sup>11</sup>

## 5. MODEL USED FOR SIMULATION

We use a simple 1-D model to compare the behavior of the different NEQ formulations shown before. The generic model basically views the x rays as being blurred when they are converted into charge or light photons. In the limit of a large number of random secondaries, the blurring can be modeled as a convolution with a Gaussian function of the following form:

$$blur(x; \sigma_b) = \frac{G}{\sqrt{2\pi}\sigma_b} \exp\left(-\frac{x^2}{\sigma_b^2}\right), \quad (19)$$

where  $x$  is the space variable (in pixels),  $G$  is the gain and  $\sigma_b$  will be used to vary the amount of presampling blur. The signals of interest will also be modeled by Gaussians, which allow us to compute the data analytically up to the evaluation of error functions:

$$\begin{aligned} s(x; \sigma_s, p, S) &= \frac{S}{\sqrt{2\pi}\sigma_s} \exp\left(-\frac{(x-p)^2}{\sigma_s^2}\right), \\ \bar{g}_m(s) &= \int_m (s * blur)(x) dx, \end{aligned} \quad (20)$$

where  $\sigma_s$  controls the signal size,  $p$  gives the location and  $S$  is the scaling constant so that the SNRs come out to a reasonable value. The numerical values used for the simulations where  $q = 10^6$  x-ray photons per pixel,  $S = 10^3$  x-ray photons per pixel and  $G = 1$  secondary per x-ray photon.

For a low-contrast signal,  $K_g$  for our model is:

$$\begin{aligned} [K_g]_{mm'} &= \langle \Delta \mathbf{g}_m \Delta \mathbf{g}_{m'} \rangle, \\ &= \int_m dx \int_{m'} dx' \int_{m'} d\tilde{x} \int d\tilde{x}' blur(x-x') blur(\tilde{x}-\tilde{x}') \langle \Delta b(x') \Delta b(\tilde{x}') \rangle, \\ &= \int_m dx \int_{m'} dx' \int_{m'} d\tilde{x} \int d\tilde{x}' blur(x-x') blur(\tilde{x}-\tilde{x}') q \delta(x'-\tilde{x}'), \\ &= \int dx' q \int_m dx blur(x-x') \int_{m'} d\tilde{x} blur(\tilde{x}-x'), \\ &= \int dx' q h_m(x') h_{m'}(x'). \end{aligned} \quad (21)$$

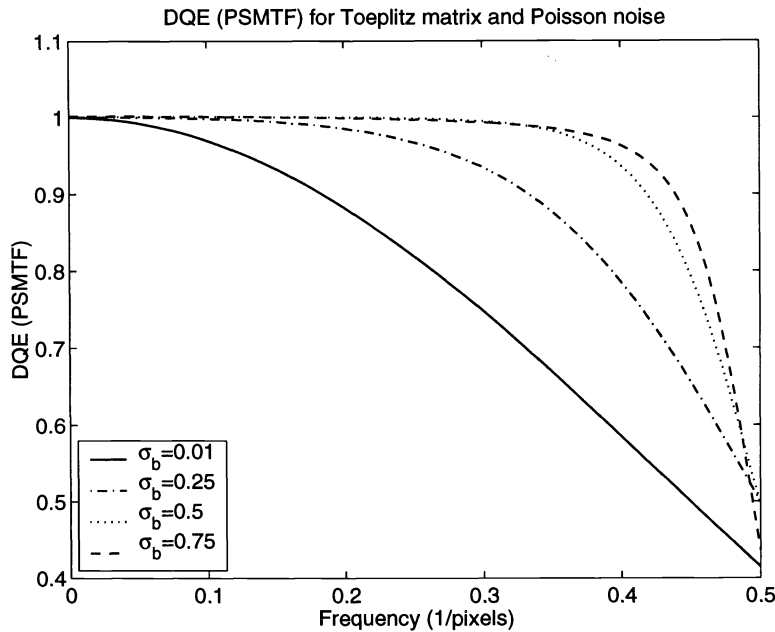


**Figure 1.** This figure shows how, with our model, the  $DQE_d$  defined using the PSMTF can improve as we increase the presampling blur. For higher amounts of blur than those shown, the DQE deteriorates.

From these formulations we can compute all the NEQ-inspired SNRs as well as the ideal observer SNR for this simple model for the case where all the variation comes from the Poisson nature of the x rays. For the case that includes electronic noise, we add a diagonal term. All the simulations assume no gap between pixels and use a detector array with 512 pixels.

## 6. SIMULATION RESULTS

The relation of the different figures of merit was studied by looking at the effect of varying the amount of presampling blur in a similar way as Rowlands et al.<sup>6</sup> Following Rowlands' paper, we can see that if we look at the case with only Poisson noise, the  $DQE_d$  given by the PSMTF improves, see figure 1. Such a result may be interpreted as saying that adding presampling blur is not only better at reducing aliasing but that it also improves overall system performance. This conclusion would be misleading.

We first look at the dependence of the SNR(ideal) on the signal location. For signals much smaller than a pixel, we see a strong dependence on location. For signals of the order of a pixel or larger, we do not see much change in the SNR ( see figure 2 ). This spatial dependence is important in terms of interpreting the results from detectability computations with negligible electronic noise. If a detectability study was done with a small signal always at the center of the pixel, it would give the impression that some presampling blur would significantly improve detectability. When we added 10% electronic noise, there was no dependence on position. In order to avoid the dependence on signal position, we will assume that signals are likely to be distributed uniformly over a pixel and average over the pixel location.

In order to carry out the comparisons between the ideal SNR and the  $NEQ_d$ , we vary the amount of presampling blur and see how the SNR changes (figure 3). If we truncate the edges of the detector, the covariance matrix for our model is Toeplitz. We find that under these circumstances, the PSMTF & DSFT (eqn. 18) formulation closely approximates the location-averaged ideal SNR ( $\langle SNR^2(ideal) \rangle$ ). The difference seen at higher presampling blurs reflects the errors in approximating the DSFT by using a replicated DFT when the covariance matrix is not circulant. As the detector increased in size, the approximation became better. For our simple model, in the limit of an infinite number of pixels in a detector the Toeplitz covariance matrix becomes circulant (figure 4).

Out of the three SNRs presented here, the PSMTF & DSFT SNR is the only one that attempts an explicit connection to lesion detectability.<sup>10</sup> The PSMTF and EMTF SNRs should not be compared in terms of their exact

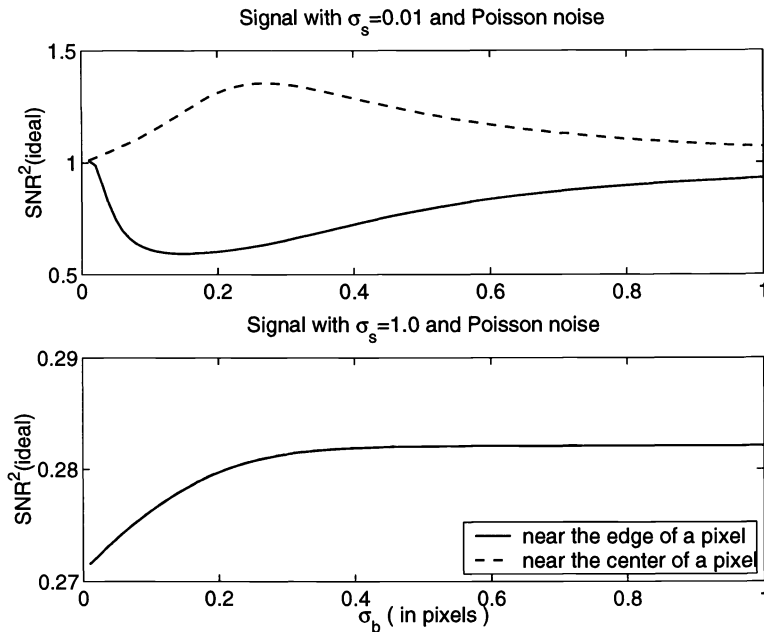


**Figure 2.** This figure shows the dependence of the ideal SNR on presampling blur with object location in the absence of electronic noise. For small signals, we see a strong dependence on signal location. For signals of the order of a pixel, there is not much change. Note the expanded scale on the second plot.

agreement with the  $\langle SNR^2(ideal) \rangle$  but in terms of the design decisions that they lead to. In particular, if we look at the Poisson noise case with a small lesion, all four figures of merit have a different behavior as we increase the presampling blur. The motivation for this work was the counterintuitive result found by Rowlands et al.<sup>6</sup> where presampling blur improved system performance. This result as seen before in the DQE (figure 1) is reproduced for this case. The  $\langle SNR^2(ideal) \rangle$ , on the other hand, remains constant.

We see that as the lesion size increases, the difference between the PSMTF & DSFT SNR and the PSMTF SNR decreases. This is because the frequency support of the signal mostly lies below the Nyquist frequency of the detector. In this case, both formulations are the same.

Not only do the design decisions vary with the SNR chosen, they also vary with the signal of interest. The design process cannot be made by separating the hardware component from the objects and optimizing it independently.

We also looked at the effect of adding electronic noise to our model by adding independent Gaussian noise with 10% of the variance of the Poisson noise to our data. The results show that for small signals the  $\langle SNR^2(ideal) \rangle$  no longer remains constant (figure 3). The ideal observer can undo the correlation arising from the detection process but not the variance from the electronic noise added after detection. For sub-pixel lesions we find that the optimal amount of presampling blur is none. Even with electronic noise, for lesions of comparable size to a pixel, presampling blur increases detectability slightly. We also see that introducing electronic noise after detection improves the approximation by the PSMTF & DSFT. Electronic noise makes the covariance matrix more diagonally dominant and hence closer to being diagonalized by the DFT.

## 7. DISCUSSION

The purpose of this paper is to explore the connection between the different formulations of the  $NEQ_d$  and the ideal SNR. The purpose was not to appropriately model a digital radiography system. In order to do so, one would have to use a 2-D model, improve the forward model and the description of the sources of variation in the data, both anatomical and from the measurement process. What we found is that if one insists, as we do, on a detectability interpretation of the SNR, the  $NEQ_d$  formulations studied here do not always correlate to detectability. Even for small amounts of presampling blur, the SNR based on the PSMTF behaves differently than the SNR(ideal). For small lesions, with and without electronic noise, the SNR(PSMTF) increases whereas the SNR(ideal) remains constant or

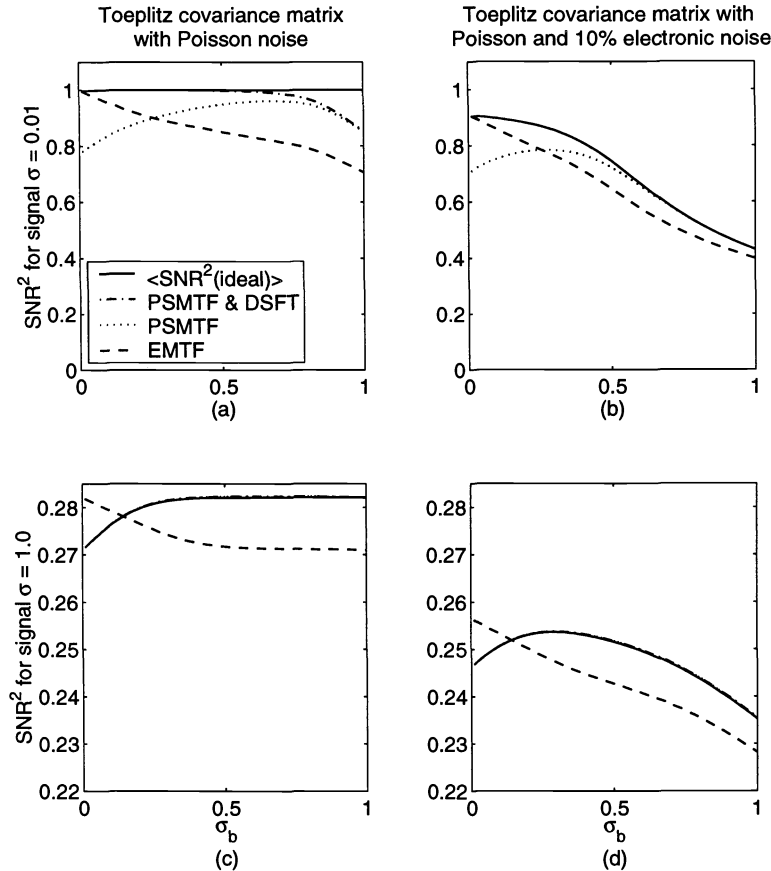


**Figure 3.** This figure shows the comparison of all the different forms of SNR. The different SNR formulations lead to different design decisions with respect to the effect of presampling blur. The behavior of the system performance also depends on the signal of interest. The SNR formulation based on the PSMTF & DSFT strays from the location-averaged ideal SNR because it bases its DSFT on replicated DFTs. When we add electronic noise, the SNR(ideal) no longer remains constant for small lesions. We also see that the PSMTF & DSFT approximation improves as the covariance matrix is more amenable to be diagonalized by the DFT. Note the expanded scale on the last row, the variation is much smaller than it appears.

decreases. This implies a fundamentally different design decision with respect to the addition of presampling blur to the imaging system. Therefore, we should use a fully digital figure of merit that avoids the pitfalls that come from trying to combine continuous and discrete representations of the imaging system.

Even the PSMTF & DSFT, which approximates the  $\langle SNR^2(ideal) \rangle$  well in many cases under this simple model, relies on estimating the PSMTF and NPS from the data. In our simulations we used the exact variance of the DFT elements as our  $NPS_d$ , the exact PSMTF and a simple model that only slightly tested the circulant nature of the covariance matrix. In more realistic models, there will be more sources of error for these tasks. It seems that trying to retain the continuous aspects of the imaging system only introduces further sources of error.

To obtain a figure of merit that depends on scale and takes into account measurement uncertainty without the use of Fourier methods, we suggest a plot of  $\langle SNR^2(ideal) \rangle$  as a function of signal size (figure 5). This quantification of system performance does not rely on shift-invariance or stationarity. As seen in figure 3 (b,d), even in the presence of electronic noise, some blur improves SNR(ideal) for some signals. Figure 5 shows just how the signal size determines whether blur is beneficial and by how much. It remains to be seen what the behavior will be for a more realistic model of digital radiography.

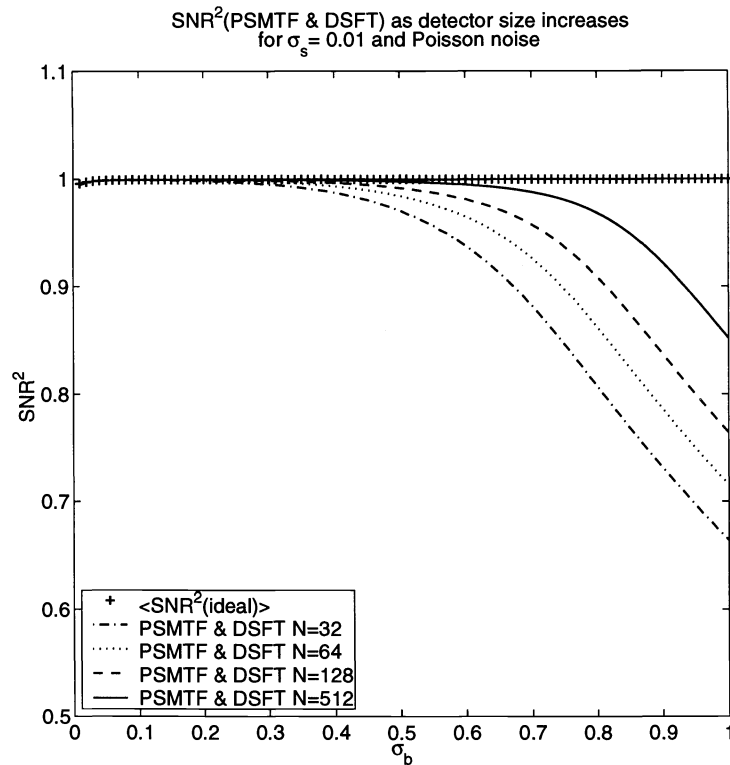


**Figure 4.** As the detector size increases, the PSMTF & DSFT approximation to the location-averaged ideal SNR improves. Even for a highly idealized detector, there still some error that comes from the estimation of the  $NPS_d$  from the data via a DFT.

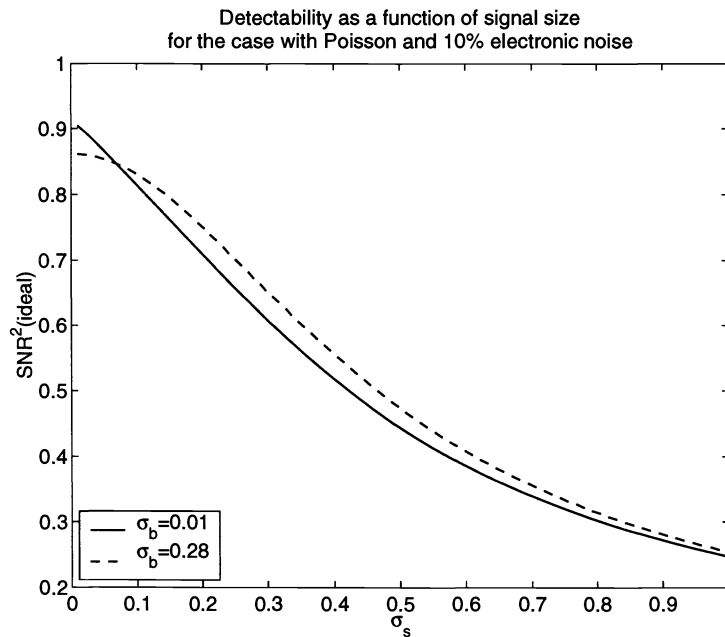


**Figure 5.** By plotting  $\langle SNR^2(ideal) \rangle$  as a function of signal size we obtain a figure of merit that depends on scale but does not rely on shift-invariance or stationarity.

## 8. CONCLUSION

From our simulations, there does not seem to be a clear advantage to sticking to a continuous figure of merit. We also find that one cannot optimize an imaging system without taking into account the objects to be imaged. If one adheres to the statistical-decision-theory interpretation of the SNR, the SNR defined from the data provides the most reliable approach to system optimization. Approximations based on the  $NEQ_d$  include further sources of error. How to actually carry out these computations for large matrices and more realistic models is shown in Barrett, et al.<sup>12</sup> and Myers et al.<sup>13</sup>

## ACKNOWLEDGMENTS

The authors would like to thank K. J. Myers, E. Clarkson, A. Lehovich and B. Wilfley for their suggestions. This work was made possible by funding from NIH grant RO1 CA52643.

## REFERENCES

1. M. L. Giger and K. Doi, "Investigation of basic imaging properties in digital radiography. 1. Modulation transfer function," *Med. Phys.* **11**, 3, pp. 287-295, 1984.
2. M. L. Giger, K. Doi and C. E. Metz, "Investigation of basic imaging properties in digital radiography. 2. Noise Wiener spectrum," *Med. Phys.* **11**, 6, pp. 797-805, 1984.
3. J. T. Dobbins III, "Effects of undersampling on the proper interpretation of modulation transfer function, noise power spectra, and noise equivalent quanta of digital imaging systems," *Med. Phys.* **22**, 2, pp. 171-181, 1995.
4. W. Zhao and J. A. Rowlands, "Digital radiology using active matrix readout of amorphous selenium: Theoretical analysis of detective quantum efficiency," *Med. Phys.* **24**, 12, pp. 1819-1833, 1997.
5. I. Cunningham, "Applied Linear Systems Theory," *Handbook of Medical Imaging Vol. 1 Physics and Psychophysics*, eds. J. Beutel, H. L. Kundell and R. L. Van Metter, SPIE Press, 2000.
6. J. A. Rowlands, W. G. Ji, W. Zhao and D. L. Lee, "Direct conversion flat panel x-ray imaging: reduction of noise by presampling filtration," *Proc. SPIE* **3977**, pp. 446-454, 2000.
7. R. F. Wagner and D. G. Brown, "Unified SNR analysis of medical imaging systems," *Phys. Med. Biol.* **30**, 6, pp. 489-518, 1985.
8. H. H. Barrett, J. L. Denny, R. F. Wagner and K. J. Myers, "Objective assessment of image quality. II. Fisher information, Fourier crosstalk, and figures of merit for task performance," *J. Opt. Soc. Am. A.* **12**, 5, pp. 834-852, 1995.
9. H. H. Barrett, J. Yao, J. Rolland and K. J. Myers, "Model observers for assessment of image quality," *Proc. Natl. Acad. Sci. USA* **90**, pp. 9758-9765, Nov. 1993.
10. M. Albert and D. A. Maidment, "Linear response theory for detectors consisting of discrete arrays," *Med. Phys.* **27**, 10, pp. 2417-2434, 2000.
11. E. Clarkson, A. R. Pineda and H. H. Barrett, "An analytical approximation to the Hotelling trace for digital x-ray detectors," *Proc. SPIE* **4320** to be published 2001.
12. H. H. Barrett, K. J. Myers, B. Gallas, E. Clarkson and H. Zhang, "Megalopinakophobia: Its symptoms and cures," *Proc. SPIE* **4320** to be published 2001.
13. R. M. Gagne, J. S. Boswell, K. J. Myers and G. Peter "Lesion detectability in digital radiography," *Proc. SPIE* **4320** to be published 2001.